Physiological Noise: Definition, Estimation, and Characterization in Complex Biomedical Signals

Andrea Scarciglia, *Member, IEEE*, Vincenzo Catrambone, *Member, IEEE*, Claudio Bonanno, and Gaetano Valenza, *Senior Member, IEEE*

***Abstract*— *Background:* Nonlinear physiological systems exhibit complex dynamics driven by intrinsic dynamical noise. In cases where there is no specific knowledge or assumption about system dynamics, such as in physiological systems, it is not possible to formally estimate noise. *Aim:* We introduce a formal method to estimate the power of dynamical noise, referred to as physiological noise, in a closed form, without specific knowledge of the system dynamics. *Methodology:* Assuming that noise can be modeled as a sequence of independent, identically distributed (IID) random variables on a probability space, we demonstrate that physiological noise can be estimated through a nonlinear entropy profile. We estimated noise from synthetic maps that included autoregressive, logistic, and Pomeau-Manneville systems under various conditions. Noise estimation is performed on 70 heart rate variability series from healthy and pathological subjects, and 32 electroencephalographic (EEG) healthy series. *Results:* Our results showed that the proposed model-free method can discern different noise levels without any prior knowledge of the system dynamics. Physiological noise accounts for around 11% of the overall power observed in EEG signals and approximately 32% to 65% of the power related to heartbeat dynamics. Cardiovascular noise increases in pathological conditions compared to healthy dynamics, and cortical brain noise increases during mental arithmetic computations over the prefrontal and occipital regions. Brain noise is differently distributed across cortical regions. *Conclusion:* Physiological noise is very part neurobiological dynamics and can be measured using the proposed framework in any biomedical series.**

***Index Terms*—Approximate Entropy, complexity, electroencephalography (EEG), heart rate variability (HRV), nonlinear analysis, noise, physiological noise.**

Manuscript received 8 March 2023; revised 22 May 2023 and 26 June 2023; accepted 28 June 2023. Date of publication 3 July 2023; date of current version 25 December 2023. This work was supported in part by European Commission Horizon 2020 research and innovation programme under Grant 101017727 through Project EXPERIENCE and in part by the Italian Ministry of Education and Research (MIUR) in the framework of the FoReLab Project (Departments of Excellence). *(Corresponding author: Andrea Scarciglia.)*

Andrea Scarciglia is with the Department of Information Engineering, School of Engineering, University of Pisa, 56122 Pisa, Italy, and also with the Bioengineering and Robotics Research Center E.Piaggio, School of Engineering, University of Pisa, 56122 Pisa, Italy (e-mail: andrea.scarciglia@phd.unipi.it).

Vincenzo Catrambone and Gaetano Valenza are with the Department of Information Engineering, School of Engineering, University of Pisa, Italy, and also with the Bioengineering and Robotics Research Center E.Piaggio, School of Engineering, University of Pisa, Italy.

Claudio Bonanno is with the Department of Mathematics, University of Pisa, Italy.

Digital Object Identifier 10.1109/TBME.2023.3291538

I. Introduction

NOISE has been accidentally discovered by Albert Einstein in 1905, when he observed that atoms move according to the Brownian molecular motion [1]. After that, noise has been brought up in countless accounts of physical and biological systems, without acknowledging its critical role and, especially, without a formal methodological framework for its definition, characterization, and exploitation. The term noise generally refers to random or unpredictable fluctuations and disturbances that are not part of the target signal or system. On one hand, the so-called measurement noise has a significant impact on all system estimates and it is considered unpredictable except for its mean, which is assumed to be zero, and its variance among repetitions. This noise, also known as *output noise*, adds up to the system output and it is supposed to not play a role in the dynamical evolution of the system. On the other hand, the *dynamical noise* is part of each integration step of a dynamical system. While its presence may be quite peculiar in a plethora of physical and biological systems, it has only been qualitatively or heuristically investigated in the nervous and cardiovascular systems [2], [3]. Also, variability induced by noise seems essential in sensory perception and movement tasks [4].

Noise in physiological systems has especially been studied in the nervous system since neural activity and related trial-to-trial variability are affected by multiple noise sources (see reviews in [3], [4], [5]). More specifically, sensory noise is intrinsically present in external stimuli and sensory receptors (e.g., thermodynamics in chemical sensing for smell), and cellular noise contributes to neuronal variability, i.e., the timing of action potentials in response to identical stimuli varies over repeated trials [6]. Electrical noise in neurons refers to stochastic changes in voltage-gated ion channels that produce millisecond variability in action-potential initiation and propagation, whereas motor noise refers to the noisy conversion of neural signals into muscular forces [7]. Furthermore, synaptic noise has been associated to noisy biochemical processes that underlie synaptic transmission; it may also be experimentally simulated by adding reasonable levels of extracellular noise to synaptic input. Such noise improves information handling by brain circuits [6], also by generating high-frequency oscillations [8]; it has been proven determinant for the detection of subthreshold signals in hippocampal neurons [9]. At a macroscopic level, noise generated by random spikes of neurons may influence brain behavior [3], and several important processes such as decision-making, or

stability of memory recall [10]. Cognitive operations are also affected by stochasticity in N-methyl-D-aspartate receptors, which may affect short-term memory [11]. Overall, noise in the brain may promote creativity and the shifting of attention to new tasks [11]. Spontaneous voltage fluctuations in the neocortex has been referred to *in-vivo* noise as their amplitude is comparable to stimulus-induced voltage modulations [12].

Regarding cardiovascular dynamics, healthy heartbeat series can be modeled as the output of a nonlinear deterministic system (e.g., the pacemaker cells of sinus node) being forced by a high-dimensional input (the activity in the nerves innervating the sino-atrial node) [13], [14], [15]. Indeed, heartbeat series show intrinsic physiological noise as the cardiovascular system is constantly involved in a dynamical, mutual interplay with numerous other physiological subsystems (e.g., endocrine, neural, and respiratory) [16], as well as in multiple self-regulating, adaptive biochemical processes [17]. In this context, it is well known that the effects of combined sympathetic and vagal stimulation on heart rate are not simply additive. This is because sympathetic stimulation inhibits acetylcholine release by acting on adrenergic receptors on the vagal terminals, cytosolic adenosine 3.5-cyclic monophosphate mediates postjunctional interactions between the sympathetic and vagal systems, and acetylcholine released by vagal stimulation inhibits norepinephrine release by acting on muscarinic receptors on sympathetic nerve terminals [17]. As a result, cardiovascular dynamics exhibits an inherently complex structure characterized by non-stationary, intermittent, scale-invariant and nonlinear behaviors [13].

The evidence above demonstrates that dynamical noise may not only significantly affect physiological system functioning, but also it is part of physiological system dynamics. Indeed, physiological systems are deemed complex dynamical systems and, particularly, nonlinear systems driven by stochastic inputs (i.e., noise) where a chaotic regime may occur [13], [14], [15], [18]. From a methodological viewpoint, to the best of our knowledge, physiological noise has not been formally defined and characterized yet. In fact, there is no effective and quantitative methodological framework able to estimate dynamical noise power in mono-dimensional or multi-dimensional physiological time series, especially when the model of system dynamics is unknown (or, at least, no assumptions are made). Previous attempts for dynamical noise estimation in complex time series have been proposed in [19], [20]. They rely on the precise estimation of the system largest Lyapunov exponent, which however should theoretically be known a priori. Besides not relying on formal mathematical proofs, these heuristic, qualitative and geometrical procedures may be severely biased by the time series behavior and parameter selection (e.g., tolerance). Moreover, they may not detect output noise level when its standard deviation (std) exceeds 10% of the signal std [20]. Other interesting heuristic methods for noise level estimation have been reported in [21], [22], [23], [24]. While works in [21], [24] focused on output noise exclusively, [22], [23] strictly focused on estimation on chaotic time series. Moreover, these approaches relied on the calculation of correlation dimension, which however may not always detect chaos (e.g., a stochastic process can have correlation dimension equal to 0 [25]).

In this work we propose a new methodological framework for estimating physiological noise in a model-free manner. Formally, consider a physiological system described by an unknown map T. We suppose that the sampled signals z_n are contaminated by physiological noise, i.e., a sequence of independent and identically distributed Gaussian random variables $\{\varepsilon_n\}_n \sim \mathcal{N}(0, \sigma^2)$ with mean 0 and fixed standard deviation σ. We aim to estimate the physiological noise $\{\varepsilon_n\}_n$ for any signal of the form $z_n = T(z_{n-1}, z_{n-2}, \ldots, z_0) + \varepsilon_n$ in closed form, without any information about the specific T function. This holds true for any continuous and differentiable T function. In this study, we consider noise as a stochastic component of a signal that modifies its dynamics and cannot be predicted from its past history. Previous works have attempted to characterize this unpredictability using non-linear information theory tools, such as conditional entropy. Especially, the logarithm of the variance of the prediction error obtained through autoregressive models when the signal of interest is modeled as a sequence of Gaussian random variables has been explored [26], [27]. To test the proposed method, we first evaluate its performance on synthetic data corrupted by dynamical noise and then apply it to experimentally gathered physiological signals. Specifically, we aim to investigate whether physiological noise can serve as an intrinsic complexity feature for cardiovascular data, such as heart rate variability (HRV) series, and cortical data, such as electroencephalography (EEG) series. Our objective is to determine whether the estimated noise varies both between (i.e., HRV vs EEG) and within (i.e., EEG channels) systems and whether it can be utilized as a potential biomarker to distinguish pathological and physiological conditions.

II. Materials and Methods

A. Physiological Noise Definition

Let us consider a physiological system as a discrete metrical dynamical system (X, μ, T). Here, X is a compact subset of $\mathbb{R}$, and T is any differentiable map function with bounded derivative, which preserves the probability measure μ. A typical noise-free output of this system is represented as $w_n = T(w_{n-1}, w_{n-2}, \ldots, w_0)$, where $w_i \in X$ for all positive integers i.

We define the *physiological noise* as a sequence of IID random variables $\{\varepsilon_n\}_n$, which constitutes the *dynamical noise*. The samples of ε_n, in fact, modify physiological dynamics at each step according to the equation:

$$x_n = T(x_{n-1}; x_0) + \varepsilon_n, \tag{1}$$

which may include generic mapping functions as $x_n = T(x_{n-1}, x_{n-2}, \ldots, x_0) + \varepsilon_n$, where $x_i \in X$ for all positive integers i, and $\{x_n(\varepsilon)\}_{n=1}^{N}$ is a noisy physiological time series that contains N samples. From the best of our knowledge, without any specific information or assumption on T, it is not possible to estimate noise ε_n formally. Let $\psi(t)$ be the Probability Density Function (PDF) of the random variable given by the difference between any two samples of the noise process. For any perturbed orbit of the system $x(\varepsilon) = (x_0, T(x_0) + \varepsilon_1, T(T(x_0) + \varepsilon_1) +$

$\varepsilon_2, \dots$), it holds [28]:

$$\mathrm{ApEn}(\{x_n(\varepsilon)\}_{n=1}^{\infty}, m, r) \approx -\log\left[2\psi(0)r\right] \tag{2}$$

for any embedding dimension $m \in \mathbb{N}$ and for a small enough tolerance r, where ApEn represents the nonlinear quantifier *Approximate Entropy* introduced by Pincus [25] to estimate the complexity/regularity in short time series. A formal definition of the ApEn is reported in the Appendix I below for the sake of completeness. Next, we introduce a formal method to estimate the ε_n power without knowledge on the specific T function, i.e., for any T function.

B. Physiological Noise Estimation

Unlike Markovian formalism, where time series points are seen as a sequence of random variables governed by transition probabilities between consecutive states, in this framework the following assumptions are made:

- The system dynamics is deterministic, taking also into account the possibility of having deterministic chaos, and ruled by any differentiable map T;
- Physiological noise samples are realization of IID Gaussian random variables $\{\varepsilon_n\}_n$ following the distribution $\psi \sim \mathcal{N}(0, \sigma^2)$;
- The system dynamics is perturbed by dynamical noise: for a noise sequence $\{\varepsilon_n\}_n \sim \mathcal{N}(0, \sigma^2)$, any orbit of the dynamical systems is of the form $x_n = T(x_{n-1}, \dots, x_0) + \varepsilon_n$

In terms of time series analysis, the properties of the map T appear the most general and suitable to describe and model a wide class of observable phenomena, as long as the systems under study is a dynamical system contaminated by random components.

Given these assumptions, and following the theory in Section II-A, the noise std σ can be approximated by the tolerance value r for which the functions $z \to \mathrm{ApEn}(\{x_n(\varepsilon)\}_{n=1}^{\infty}, m, z)$ and $z \to -\log z$ show the most similar differential behavior. Then (2) becomes:

$$\mathrm{ApEn}(\{x_n(\sigma)\}_{n=1}^{\infty}, m, r) \approx -\log\left[r/(\sigma\sqrt{\pi})\right]$$

Therefore, we can derive the power σ of physiological noise in a closed form as follows:

$$\log(\sigma) \approx \mathrm{ApEn}(\{x_n(\sigma)\}_{n=1}^{\infty}, m, r) + \log(r/\sqrt{\pi})$$

Here, j is a time index, m is the embedding dimension, τ is the delay-time for state-space reconstruction, and $N + (m-1)\tau$ is the time series cardinality when $r < \sigma$ and $r \to 0^+$.

1) Estimation Algorithm: Under the previous reasonable assumptions, dynamical noise power σ^2 estimation can be performed as follows:

- Consider a noisy series X composed by N samples;
- Fix an embedding dimension m;
- Estimate the profile map $r \to \mathrm{ApEn}(X, m, r)$ as function of the tolerance parameter r. The parameter r varies from 0 to the amplitude of the series X with an arbitrary Δr step;

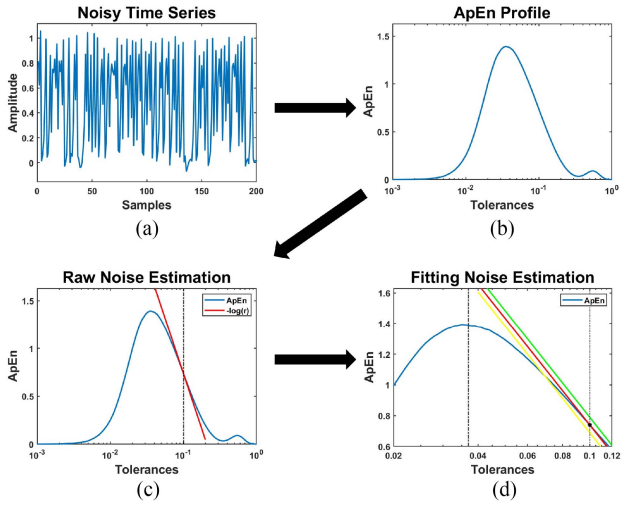

Fig. 1. Dynamical noise estimation procedure: take a noisy series as input (panel (a). First, the function $r \to \mathrm{ApEn}(X, m, r)$ is estimated (panel (b) - r ranging between 0 and the series amplitude with a Δr step. A first, raw noise power estimation is performed by searching for the point in which the ApEn profile and the curve $-\log r$ (red line) have the same slope (panel (c)). According to the corollary, an improved std estimation is then performed by a curve fitting procedure with respect to the curve $\sigma \to \mathrm{ApEn}(X, m, r) + \log\left[r/(\sigma\sqrt{\pi})\right]$, in the tolerance interval $I(\bar{r}) = [r_{\max}, \bar{r}]$ (delimited by vertical dashed lines), where noise is supposed to be seen (panel (d)).

- A first std σ is estimated by searching for the tolerance value $\bar{r}$ which minimizes the discrete derivative of $r \to \mathrm{ApEn}(X, m, r) + \log r$;
- Choose a neighborhood $I(\bar{r})$ of $\bar{r}$ and find the best fit $\bar{\sigma}$ for the function $\sigma \to \mathrm{ApEn}(X, m, r) + \log\left[r/(\sigma\sqrt{\pi})\right]$.

A suitable choice of $I(\bar{r})$ might be $I(\bar{r}) = [r_{\max}, \bar{r}]$, where $r_{\max}$ denotes the tolerance value in which $r \to \mathrm{ApEn}(X, m, r)$ reaches its maximum. The estimation algorithm is illustrated in Fig. 1. We focus our attention on the noise estimation algorithm's description, limiting our analysis to the interval $I(\bar{r})$, which spans from the point of maximum for ApEn to the point with the most similar slope to the curve $r \to -\log r$. This approach ensures that we avoid using corrective terms for the ApEn [29] in situations where we have only (or mostly) self-matches, specifically tolerance values between 0 and the maximum point. It also prevents the introduction of erroneous noise effects and the creation of additional spurious points with a slope similar to the curve $r \to -\log r$.

To enhance the efficiency of the approximate entropy algorithm [25], we employ the Cumulative Histogram Method (CHM) [30] instead of executing the ApEn algorithm for each tolerance value of the uniform grid. The CHM method eliminates the need for consecutive runs of the ApEn entropy algorithm, which has a quadratic time complexity of $O[n^2]$ for each tolerance value r, where n is the length of the time series. The CHM computes the ApEn profile efficiently in a single run, regardless of the number of tolerance radii, by utilizing cumulative histograms.

C. Experimental Data

1) Synthetic Data: The proposed noise estimation method was tested on the following analytical benchmarks:

– *Logistic maps:* a family of maps described by the equation

$$f_\lambda : [0,1] \to [0,1], \quad f_\lambda(x) = \lambda x(1-x)$$

where λ is a real parameter in the interval [0,4]. Simulation are performed with $\lambda = 4$, i.e. in chaotic regime (Kolmogorov-Sinai entropy > 0).

– *Pomeau-Manneville maps:* a family of chaotic maps described by the function

$$T_\alpha : [0,1] \to [0,1], \quad T_\alpha(x) = \{x + x^\alpha\}$$

where α is a real number greater than 1, and the braces denote the reduction modulo 1. For each α, there exists only one T_α-invariant measure μ_α. In addition, the probability measure $\mu_\alpha([0,1])$ is finite for $1 < \alpha < 2$, and infinite for $\alpha \geq 2$ [31]. Particularly, we took into account Pomeau-Manneville maps with $\alpha = 1.8$, almost close to the threshold $\alpha = 2$, where the absolutely continuous probability measure leading is not preserved by the map.

– *Autoregressive model:* the series of an autoregressive model of order p, denoted as AR(p), can be expressed by the following equation:

$$y_n = \sum_{i=1}^{p} a_i y_{n-i} + \varepsilon_n \tag{3}$$

where y_n is the n-th observation in the time series, a_i are the p constant coefficients, and ε_n is an IID Gaussian random variable, also known as the innovation process. For our analysis, we have chosen an AR(7) model with the following parameter values: $a_1 = 1.046$, $a_2 = -0.219$, $a_3 = 0.105$, $a_4 = 0.033$, $a_5 = -0.0885$, $a_6 = -0.136$, $a_7 = 0.105$. These values were obtained by fitting the Yule-Walker equations to an exemplary Heart Rate Variability series of a healthy subject from the NS cohort (the first series, as described in the next subsection). The choice of an autoregressive model of order $p = 7$ is justified by its importance in computational physiology. Autoregressive models enable the characterization of time series regularity in terms of conditional entropy and the variance of the innovation process, particularly when the time series are regarded as Gaussian random variables from an autoregressive model [26].

For Logistic and Pomeau-Manneville maps, synthetic time series have been generated by superimposing dynamical noise as follows: fixed an initial condition $\bar{x}$, it was exploited to produce a noise-free series of 20000 samples; then, a realization of a white Gaussian process (20000 samples) with a std equal to a percentage of the amplitude of the noise-free series was considered; finally, restarting from $\bar{x}$, the perturbed series was constructed by adding a sample of the noise realization at each step of the map equation.

We considered noise std percentages $2\%, 5\%, 10\%, 15\%, 20\%$ with respect to the time series amplitude. For each noise level and parameter 100 perturbed series were obtained. Specifically, a *bounce effect* was considered for Logistic maps simulations: when an element of the series exceeded the interval [0,1], it was forced in the interval [0,1] trough reduction modulo 1. As a consequence, it must be considered that *bounce effect* might result in actual noise std to be lower than the theoretical imposed one. The *bounce* effect is automatically verified by the reduction modulo 1 in Pomeau-Manneville maps definition.

To evaluate the performance of the AR(7) model, we generated 500 synthetic time series, each with 20000 samples. We used Gaussian innovation (also known as dynamical noise) with standard deviations of 0.5, 1, 1.5, 2, and 2.5 to create 100 realizations of the autoregressive model for each standard deviation value. To estimate the noise in the synthetic data, we used an embedding dimension of $m = 2$ and a radius step of $\Delta r = 0.001 \times \mathcal{R}$, where $\mathcal{R}$ denotes the time series range. These parameters were chosen to ensure a reliable estimation of the noise level.

2) Cardiovascular Variability Series: The proposed noise estimation methodology was tested on long-term heart rate variability (HRV) series from three datasets, publicly-available on *physionet.org* repositories [32], and specifically the MIT-BIH database for healthy subjects (https://physionet.org/content/nsrdb/1.0.0/), Congestive Heart Failure RR datasets [33] (available at https://physionet.org/content/chf2db/1.0.0/) and MIT-BIH Atrial Fibrillation database [34] (and https://physionet.org/content/afdb/1.0.0/) [32], [35].

More in detail, the first database comprised of 18 healthy subjects (age range 20–50 yo, with ECG sampled at 128 Hz) with normal sinus rhythms (NS data), the second dataset counted 29 HRV series gathered from subjects with congestive heart failure (CHF data) (24-hours Holter recordings sampled at 128 Hz, 34–79 yo), and the third dataset comprised of 23 HRV long-term (i.e., 10-hour ECG series sampled at 250 Hz) series gathered from subjects with atrial fibrillation (AF dataset). Further details on experimental recordings are available on the relative web pages.

HRV series were derived from ECG signals through the well-known Pan-Tompkins algorithm for the identification of R-peaks [36], and visually inspected for artifacts which were eventually corrected through a point-process-based method [37]. To avoid any potential bias associated with the series length, an artifact-free 10000-samples segment was selected for each subject. This study was approved by the committee of bioethics of the University of Pisa with review n. 19/2021.

Significant differences for group-wise statistics are established through not-parametric Kruskal-Wallis test with threshold $\alpha = 0.05$, with null hypothesis of equal median among all the cohorts; post-hoc pairwise comparisons are performed, instead, through non-parametric Mann-Whitney test, with threshold $\alpha = 0.05/3 \approx 0.01$ and null hypothesis of having equal median between two groups. Moreover, in order to test the robustness of the method, we employ a conservative surrogate data analysis with null hypothesis of not having physiological noise. In this context, for any time series, we generated 50 surrogate data series using random permutations, where the system dynamics is destroyed. We reject the null hypothesis when the noise level for the original series is before the 2.5-th and after the 97.5-th

percentiles of the noise distribution for its surrogate data. Of note, given that noise levels typically increase in series with destroyed dynamics, as one would intuitively expect, employing a one-tail surrogate data approach can also effectively serve as a means to assess the method's robustness.

Previous studies [2] have shown that the three cohorts exhibit different complexity levels as measured by an entropy measure over multiple scales, specifically, the multiscale sample entropy, which measures the regularity of the series at various time lags. The results indicate that for time scale one, the complexity measures for the healthy cohort were smaller than those for the remaining two cohorts. However, this trend is inverted for higher time scale factors, indicating a change in complexity. This change in complexity is also supported by other quantifiers, such as symbolic entropy [38].

Noise estimation for HRV data have are performed with an embedding dimension $m = 2$ and a $\Delta r = 0.001 \times \mathcal{R}$.

3) Electroencephalography Signals: The proposed noise estimation methodology was further tested on a publicly available EEG series dataset, namely the *EEG During Mental Arithmetic Tasks* [39]. This dataset is comprised of EEG gatherings from 36 healthy volunteers undergoing a 180 s resting phase and a 60 s mental cognitive workload task (i.e., performing mental arithmetic). Recordings from four subjects were rejected after visual inspection owing to gross artifacts. Thus, data from 32 persons (24 females) with ages of 18 ± 2.01 yrs on average were retained for further processing. The electrophysiological signals were sampled at $500\,\mathrm{Hz}$. The eligibility criteria were normal or corrected–to–normal visual acuity, normal color vision, no clinical manifestations of mental or cognitive impairment, and no learning disabilities. The use of psychoactive medication, drug or alcohol addiction, and psychiatric or neurological complaints were considered as additional exclusion criteria. Power line notch (50 Hz) and $[0.5Hz$–$45Hz]$ band–pass filters were applied in the EEG series before independent component analysis, and were used to identify artifacts (i.e., eyes, muscles, and cardiac pulsation) that were subsequently rejected. Further details on signal acquisition and preprocessing can be found in [39]. For each EEG series, outlier samples over the 98th percentile were not retained for further processing. To avoid bias associated with the series length, it is important to note that the length of the time series can affect the accuracy of noise estimation [28]. Therefore, we chose to focus on the central minute of the 180-second resting state recordings to minimize the impact of any potential noise caused by transitions to and from rest. For each channel and task, the EEG series contained 30000 samples. For any of the 19 scalp channels, Wilcoxon statistical test ($\alpha = 0.05$), with null hypothesis of having equal median between the noise levels computed in resting and computational tasks, is used to assert the significance for different levels of noise together with the Bonferroni-Holm correction for p-values [40]. The robustness of the method has been also tested with a surrogate data approach, following the same procedure as the HRV dataset. To estimate the noise level in the EEG data, we used an embedding dimension of $m = 5$ and a time delay of $\Delta r = 0.001$ times the range of the time series.

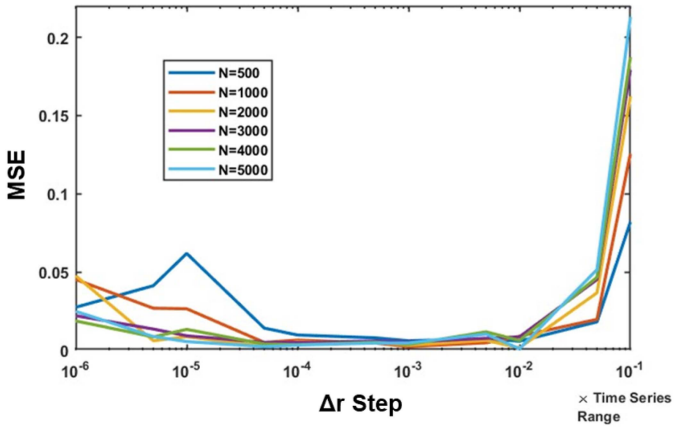

Fig. 2. Effect of Δr choice on noise estimation. We evaluated the performance of the noise estimation algorithm with different choices of Δr, ranging from 10^{-6} to 10^{-1} times the range of the time series. Specifically, we computed the mean squared error (MSE) between the estimated noise level (using embedding dimension $m = 2$) and the actual imposed noise for 10 different realizations of an AR(7) model with Gaussian innovation standard deviation equal to 1, and series lengths of 500, 1000, 2000, 3000, 4000, and 5000 samples.

Previous studies showed that higher gamma activity is associated with mental stress tasks, while alpha band were mainly present at resting state; from a time-domain analysis, it has been seen that fractal measures are capable of better differentiating signals between rest and task phases [41].

The exploitation of the dataset for this work was approved by the committee of bioethics of the University of Pisa with review n. 19/2021.

III. Experimental Results

A. Numerical Examples on Analytical Maps

Firstly, we demonstrate the importance of selecting an appropriate tolerance step Δr for the noise estimation algorithm used with both synthetic and physiological data. In particular, we propose to set $\Delta r = 0.001 \times \mathcal{R}$, where the time series range $\mathcal{R}$ refers to the difference between the maximum and minimum values in the series. Choosing the correct value of Δr is crucial as it impacts both the accuracy of the ApEn profile characterization and the computational cost of the algorithm. When a large number of samples are available, a smaller Δr leads to a more precise characterization of the profile. However, physiological recordings are often related to short time window and to a limited number of samples. To support our proposal, we performed a series of experiments using 10 realizations of the AR(7) model with Gaussian innovation standard deviation equal to 1. We varied the length N of the time series from 500 to 5000, and computed the mean squared error (MSE) between the estimated noise and the actual noise imposed with embedding dimension $m = 2$ and different tolerance steps of orders of magnitude $\Delta r = \{10^{-6}, 10^{-5}, 10^{-4}, 10^{-3}, 10^{-2}, 10^{-1}\} \times \mathcal{R}$. Fig. 2 shows that the MSE is minimized when Δr falls within the range $[0.001, 0.01] \times \mathcal{R}$, independently of the length N of the time series. Taking into account computational complexity, storage limitations, and machine constraints, we recommend setting

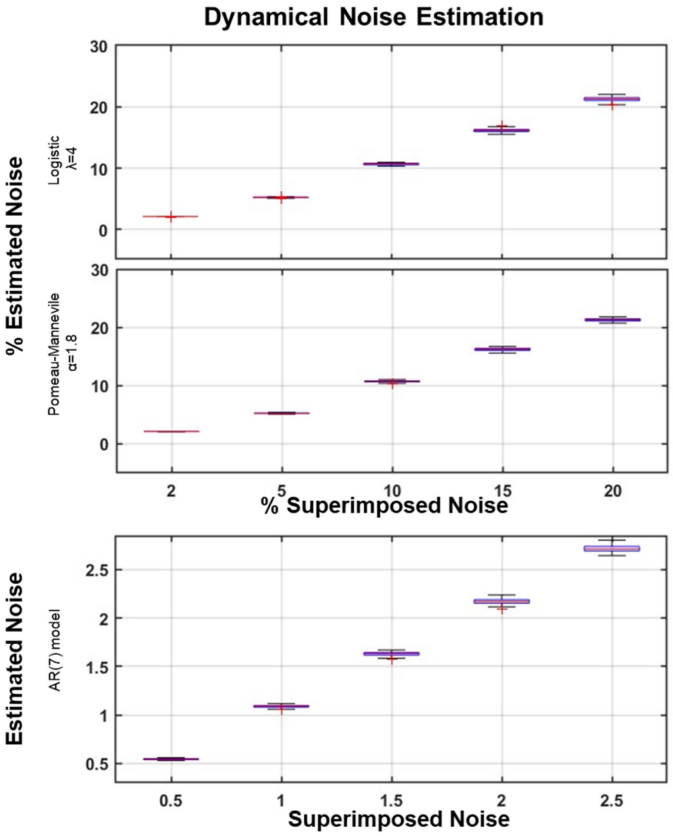

Fig. 3. Noise estimates in synthetic data. For each superimposed noise level (x-axis) noise was estimated with $m = 2$, $\Delta r = 0.001 \times \mathcal{R}$ on 100 realizations for Logistic map with $\lambda = 4$ (top panel), Pomeau-Manneville maps with $\alpha = 1.8$ (middle panel), and an AR(7) model (bottom panel). Levels of superimposed and estimated noise for the autoregressive model are expressed in terms of actual standard deviation of the Gaussian innovations.

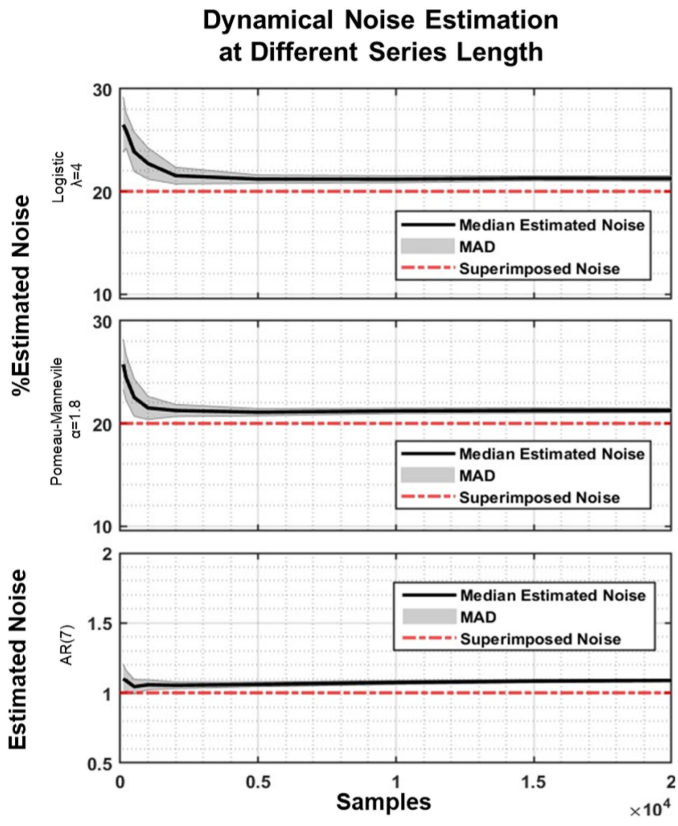

Fig. 4. Noise estimates at different series length expressed as median (black line) ± median absolute deviation (MAD) (shaded area) among 100 realizations for Logistic map with $\lambda = 4$ (top panel), Pomeau-Manneville maps with $\alpha = 1.8$ (central panel), and an AR(7) model (bottom panel). Estimates are performed with embedding dimension $m = 2$. The red dotted line indicates to the superimposed noise (20% of the noise-free series amplitude for Logistic and Pomeau Manneville maps; 1 for the AR realizations, which corresponds to the actual imposed innovation standard deviation).

$\Delta r = 0.001 \times \mathcal{R}$. Next, numerical results of the proposed noise estimation method are showed as boxplots in Fig. 3. In the case of Pomeau-Manneville and Logistic maps, it is possible to see how the proposed method discerns and estimates the different levels of noise with minimal variance across multiple repetitions, up to the limit case of disturbance as high as 20% of the time series amplitude. We observe that, even in deterministic chaotic regime, the method provides a good resolution for the noise levels variations (e.g. from %2 to %5). We also notice that the higher the level of superimposed noise, the more consistent is the dispersion around the median value, even if such a spreading is not large. The same pattern holds true for autoregressive models, where the dynamics are not limited to the interval [0,1]. As the level of noise decreases, the various levels of absolute noise can be identified with greater precision. To provide a sense of the magnitude of the estimated noise levels, it is worth noting that the imposed noise standard deviations are roughly half of the time series' standard deviation.

Fig. 4 reports experimental results gathered from noise estimation level over simulated series with several different lengths. Notice that the proposed methodologies perform reasonably well with $250 - 500$ samples for Logistic, Pomeau-Manneville maps and the AR(7) model (in this case the estimation reaches the imposed level more quickly). Although the estimation error is not negligible for short series, the estimate is maintained stable with any number of samples greater than 1000. Anew, the method appears stable across repetitions, having low variability (shaded area in Fig. 4).

B. Heart Rate Variability Series

Noise estimates from cardiovascular activity series are summarized in Fig. 5. Cardiovascular pathologies modulate underlying physiological noise, particularly increasing in AF group $(13.56\% \pm 5.98\%)$ and CHF group $(11.67\% \pm 1.93\%)$, with respect to healthy NS group $(7.85\% \pm 1.39\%)$ heartbeat dynamics. Moreover, cardiovascular noise reaches about 50% of HRV series standard deviation in case of AF $(64.5\% \pm 24.9\%)$ and CHF $(54.74\% \pm 10.69\%$ with respect to healthy subjects $(35.5\% \pm 7.18\%)$. Interestingly, groups differ in median values as well as in dispersion, with NS group being close to the median value, and the other two having higher inter-subject variability, more accentuated in AF group. Group-wise statistics confirmed significant differences through not-parametric Kruskal-Wallis

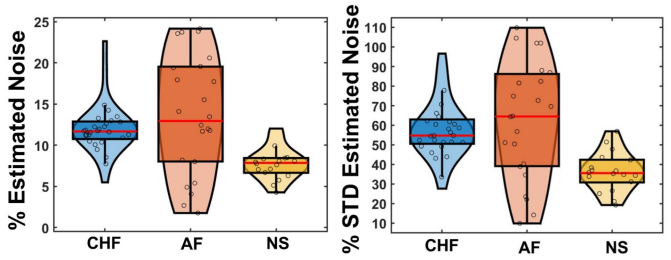

Fig. 5. Noise estimation in cardiovascular variability series. Boxplots statistics for the proposed physiological noise estimation in CHF, AF, and NS groups with embedding dimension $m = 2$. In the left panel, noise estimates are standardized with respect to the signal range, whereas in the right panel, noise estimates are normalized by the series standard deviation. Red horizontal lines indicate group median values, whereas circles indicate the single-subject estimate, and the violin plot denotes the estimate's density across central values.

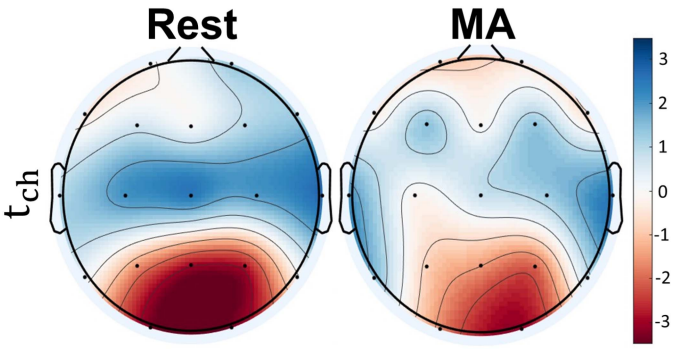

Fig. 6. Topographical representation of EEG noise distribution during the resting state and mental arithmetic task. Normalized median values across subjects as t-scores across channels using an embedding dimension $m = 5$.

test (p-value < 0.00298), whereas post-hoc comparisons performed through non parametric Mann-Whitney test confirmed main differences between CHF and NS groups (p-value < 0.0095), and between AF and NS groups (p-value < 0.0031). Furthermore, the application of surrogate data analysis has effectively verified noise as a discriminant statistic for the entirety of the HRV series. This conclusion is drawn from the rejection of the null hypothesis stating that the original and surrogate series possess equal noise levels.

C. EEG Data

Experimental results on noise estimates from EEG series are here reported. Firstly, Fig. 6 reports a topographical representation of noise estimates across the scalp during resting and mental arithmetic states. More specifically, the represented values refer to a t-score normalization performed across channels to see if significant variation were present across different scalp locations. For each channel, the value has been averaged across subjects. From this representation it is possible to appreciate that occipital and posterior parietal channels have the highest cortical noise, compared to the central electrodes, which have the lowest. In addition, right hemisphere seems to have extreme variation, with both the highest value on the posterior scalp, and the lowest on the temporal lobe.

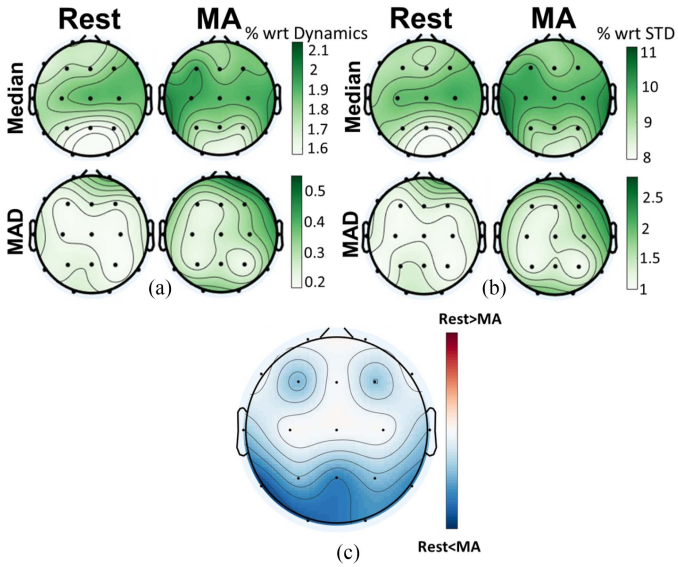

Fig. 7. Topographic representation of EEG noise estimations and statistical comparison.(a)–(b) Median (top row) and median absolute deviation (MAD) (bottom row) cortical noise levels across subjects during the resting state (left column) and the mental arithmetic (MA) task (right column). The colorbar in panel (a) represents the standardized noise estimations expressed as percentage with respect to the range of the series. In panel (b) the colorbar represents the percentage of estimated noise normalized with respect to the standard deviation of the series. (c) The topographical representation shows the corrected p-values obtained from the non-parametric Wilcoxon test for paired samples. White areas indicate non-significant differences, and blue color indicates higher noise during the MA task. The statistical significance is set at $\alpha = 0.05$, and darker areas represent lower p-values.

Variations between experimental phases are also represented in Fig. 7. In particular Fig. 7(a) and (b) illustrate a topographical representation of median (top panels) and median absolute deviation (bottom panels), calculated across subjects, for both experimental conditions, i.e., resting state (left column) and mental arithmetic (right column), with embedding dimension $m = 5$. Fig. 7(c) shows results from the statistical comparison performed through non-parametric Wilcoxon test for paired samples, where p-values were corrected for multiple comparison in accordance with Bonferroni-Holm criterion [40]. Mental arithmetic task is associated with higher neuro-physiological noise levels with respect to the resting state, especially in the prefrontal and occipital regions. Cortical noise comprises about 1.5–2% of EEG dynamics (about 8–11% of signal standard deviation) group-wise. Tasks differ in median values as well as in dispersion, with mental arithmetic associated with higher inter-subject variability over the frontal, right temporal, and occipital regions. The surrogate data approach provides compelling evidence that physiological noise can be used as a discriminating statistic for all EEG recordings. This is achieved by rejecting the null hypothesis that the original and surrogate series have equal noise levels.

D. Complexity vs. Dynamical Noise Power

Another crucial point we wish to emphasize is the independence between the estimated dynamical noise and the

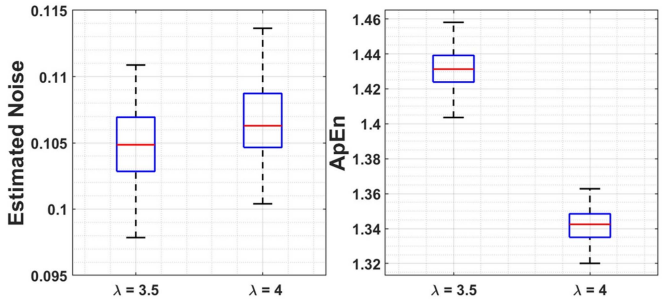

Fig. 8. Impact of Complexity on Noise Estimation. The left-hand side of the figure presents boxplots illustrating absolute noise estimations for 100 Logistic maps with varying complexity levels: periodic ($\lambda = 3.5$ and K-S entropy of 0) and chaotic ($\lambda = 4$ and K-S entropy greater than 0). The estimations were performed using an embedding dimension of $m = 2$ and a mean 0, Gaussian dynamical noise with a standard deviation of 0.1. Surprisingly, the estimated noises are almost indistinguishable, regardless of the complexity of the underlying system. On the right-hand side, boxplots display the complexity values of the same series using the ApEn quantifier with $m = 2$ and a radius equal to $0.2 \times$ std(series), representing a general setting.

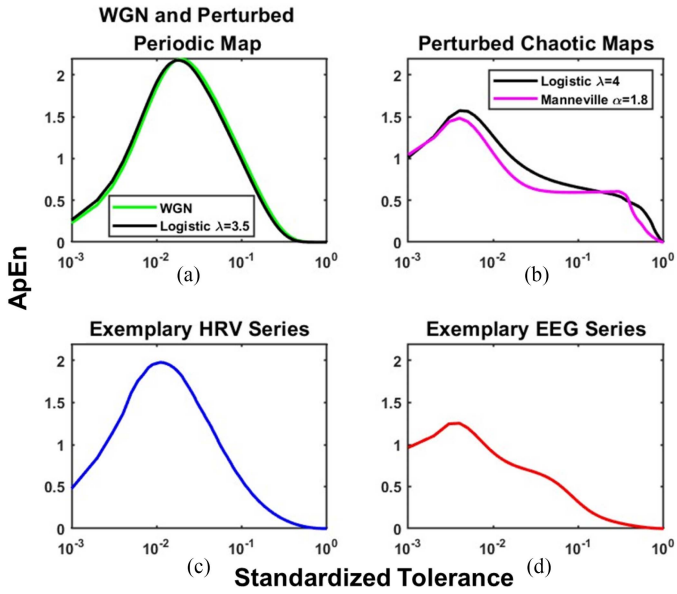

Fig. 9. ApEn profiles for synthetic and physiological series. The ApEn curve is represented as function of the tolerance parameter, standardized with respect to the series amplitude, with embedding dimension $m = 2$. Panel (a): ApEn profiles of a realization of white Gaussian noise (WGN), and of a Logistic map in periodic regime ($\lambda = 3.5$). Panel (b): ApEn profiles of a chaotic Logistic ($\lambda = 4$) and a Pomeau-Manneville map ($\alpha = 1.8$). All synthetic time series are corrupted by dynamical WGN $\sim \mathcal{N}(0, \sigma)$, being $\sigma = 5\%$ of noise-free amplitude. Panel (c): ApEn profile of a time series gathered from the HRV-NS cohort. Panel (d): ApEn profile of an EEG series gathered from resting state.

complexity of the underlying system dynamics. This fact is clearly demonstrated in Fig. 8, where we conducted noise estimations on 100 series, each consisting of 5000 samples obtained from two different Logistic maps. The first set of series is derived from the Logistic map with a parameter value of $\lambda = 3.5$, while the second set is generated by the Logistic map with a parameter value of $\lambda = 4$. In both cases, a Gaussian dynamical noise with a mean of 0 and a standard deviation of 0.1 was added. Furthermore, we evaluated the complexity of these time series using the approximate entropy quantifier with an embedding dimension of $m = 2$ and a tolerance value r set to the standard value of $0.2 \times$ std(series) [25]. On the left-hand side panel, as anticipated, we observe that noise estimations for the two groups of series show no significant differences. However, on the right-hand side panel, we discover that the conventional use of ApEn fails to capture the complexity of the underlying dynamics in the presence of noise perturbations. Surprisingly, it appears that the first series is more complex than the second, which is not the case.

IV. Discussion

We introduced a formal definition, estimation, and characterization of physiological noise. Our proposed methodology is based on the ApEn quantifier, which exhibits distinctive behavior under stochastic perturbations [28]. Such perturbations can significantly affect complex biological systems and may bias complexity estimates (e.g., entropy), therefore the resulting dynamical noise quantification can carry valuable information on the system under study. We define noise as the random component of a system's dynamics and develop methods for estimating and characterizing it. We make the assumption that the noise $\{\varepsilon_n\}$ follows a Gaussian distribution with a mean of zero, and we proceed to estimate its standard deviation. However, it is important to note that the proposed framework is not reliant on the specific nature or statistical distribution of the noise. In other words, the definition of noise does not necessitate prior knowledge or information, and it remains applicable regardless of the underlying dynamical complexity of the system. Indeed, the proposed methodology provides an effective, non-heuristic estimation of dynamical noise in every kind of mono-dimensional time series with unknown underlying dynamical system, like any physiological system.

To evaluate the correctness and robustness of our methodology, we subjected Logistic and Pomeau-Manneville maps in the chaotic regime and in the folding of the modulo 1, as well as an autoregressive model of order 7, to different levels of white Gaussian noise. The latter is of particular interest in computational physiology since it allows us to easily compute regularity quantifiers, such as the conditional entropy, while not restricting the dynamics range under noisy perturbation. Our numerical results demonstrate that our method is capable of accurately discerning and estimating the various levels of superimposed noise, with minimal variance detected across repeated estimates. Furthermore, we found that our approach is robust even for time series with more than 250 samples. Regarding noise detectability, previous research has demonstrated that the presence of noise in a time series leads to a distinctive peak in the profile of Approximate entropy as a function of the tolerance parameter [28]. Consequently, whenever the approximate entropy associated with a time series exhibits a peak (refer to Fig. 9), we can infer that the time series is influenced by dynamical/physiological noise. The proposed methodology can then be applied to accurately estimate the power of such perturbations.

This observation holds true for all the series analyzed in this study, including both synthetic and physiological datasets.

On the other hand, the relevance of the noise level necessitates a more nuanced discussion. When considering noise as a measure of the complexity of a series, it is not appropriate to classify a certain level of noise as negligible. This is because we are assessing the impact of intrinsic/dynamical perturbations, rather than external perturbations on the output. In situations where the encountered noise levels are significantly smaller than the range of the series, noise may produce trajectories that closely resemble the unperturbed ones, leading to the perception of negligible noise. However, in the context of intrinsic perturbations, even small disturbances can have a profound and irreversible effect on the dynamics of the series. A notable example is the impact of innovation processes on AR(p) models characterized by regular and deterministic dynamics: even small noise variances, relative to the series range, can completely alter the resulting trajectory. Therefore, the estimated noise levels, even if of small magnitude, should always be considered as an indication of stochastic and irreversible changes within the underlying (unknown) dynamics.

Furthermore, we tested the proposed methodology on physiological data to investigate if physiological noise varies between systems (cardiovascular, recorded as HRV series, and cerebral, gathered as EEG), within systems (different EEG locations), across pathological conditions (healthy subjects vs cardiovascular patients), and across physiological states (resting state vs experimental elicitation). Our results demonstrate that physiological systems are significantly driven by noise. As shown in Fig. 9, noise seems to change the underlying dynamics by generating peaks in the ApEn profile. Qualitatively, by comparing the four panels, it can be observed that the dynamics of HRV series might be more similar to a periodic series corrupted by noise (panels a-c), while the EEG ApEn profile simulates a structure more similar to chaotic systems due to the presence of a positive *plateau*, broken by the presence of noise (panels b–d). Quantitatively, we normalize the absolute estimate of noise standard deviation with respect to the series range, as well as with respect to the series standard deviation.

Group-wise, noise comprises approximately 1.5–2% of the EEG dynamics (i.e., about 8–11% of standard deviation) and approximately 5–10% of heartbeat dynamics (i.e., about 30–40% of standard deviation), being modulated by mental states and pathological conditions.

Focusing on HRV analysis, results suggest that cardiovascular noise is significantly modulated by pathological conditions with respect to a healthy state. Indeed, atrial fibrillation or congestive heart failure generate noisier cardiac dynamics than healthy controls, which also present much lower inter-subject variability. This indicates that cardiac pathology may modulate underlying physiological noise rather than underlying system complex dynamics. These findings are consistent with previous evidence linking low signal-to-noise ratio and dynamics resembling white Gaussian noise in cardiac disorders [2]. Further research should then investigate the reliability of complexity modulation (e.g., entropy) in cardiovascular dynamics in different experimental cases [13].

Regarding the neuro-physiological dynamics, the noise evaluation suggests a spatial distribution of noise across the scalp (see Fig. 6). Similarly to the distribution of the EEG alpha power in the resting state, occipital regions show a higher level of noise, while central electrodes have a lower level. Moreover, significant differences were detected among experimental conditions. The mental arithmetic task was associated with higher noise levels on posterior scalp areas and left prefrontal locations than in the resting state. This finding suggests that the mental arithmetic task not only modulates cortical dynamics but also modulates the underlying neurophysiological noise, targeting specific brain areas in the prefrontal and occipital regions. The increase in noise levels detected during the mental arithmetic task might be physiologically correlated to a significant fluctuation of hemoglobin oxygen levels in the brain during cognitive tasks [42] or to the alpha rhythm decrease in the parieto-occipital regions [43]. Speculatively, the significant loss of alpha rhythm might reveal an aperiodic and noisy component that is no longer covered by the alpha-wave.

Next, we discuss potential biological origins of the physiological noise observed in cardiac and cerebral systems. A link between the level of noise in neural circuits and the activity of the norepinephrine system, which is part of the sympathetic nervous system, has been established [44]. It is not surprising that such sympathetic activity and, thus, neurocardiac noise may be modulated by cognitive states [44], as the sympathetic system is part of the autonomic nervous system that innervates all body organs and systems, including the cardiovascular system. This neural control of cardiac activity is part of the central-autonomic network, which means that noise may affect the dynamics of the brain and body as a whole, including interconnected networks [18], [45]. The combined neural control of heartbeat activity through acetylcholine, cytosolic adenosine 3,5-cyclic monophosphate, and other mediators of postjunctional interactions between the sympathetic and vagal systems may result in neurocardiovascular noise [17]. Since neurocardiac noise increases with pathology, the related modulation of heart rate variability complexity should be re-evaluated. EEG originates from the activity of pyramidal neurons in the cortex and seems to be associated with a relatively high physiological noise level, whose distribution varies across the scalp. Multiple factors may influence its presence, including but not limited to, neurovascular coupling, neuro-glia interactions, and related calcium dynamics, as well as vascular motion due to heartbeat dynamics.

The limitations of this work are mainly associated with the limited parameter space spanned. Future attention will be devoted to a detailed exploration of all parameter spaces and investigating other physiological signals and systems (e.g., electromyography, electrocardiography, fMRI) and physiological correlates of estimated noise variations in patho-physiological conditions.

From the simulations shown in Section III-D, we can deduce that noise can impact the underlying system dynamics independently, without necessarily altering the system's complexity. Nevertheless, stochastic perturbations have the potential to introduce biases in complexity estimates, resulting in changes to the entropy of a time series. These changes can arise from

alterations in the system's complexity, the underlying dynamical noise, or a combination of both. Therefore, the estimated noise remains largely unaffected by the complexity of the underlying dynamics. However, the ApEn complexity quantifier proves unreliable in capturing the true complexity of the series dynamics under noisy perturbations, leading to misleading complexity characterizations.

Hence, it is essential to consider noise estimation when assessing the complexity of a time series.

V. Conclusion

This study demonstrates that physiological noise exists and may be quantified through the analysis of physiological time series. Such noise is associated with its own physiological and pathophysiological signatures. We demonstrate that the presence of physiological noise may affect measurements and evaluations in cardiovascular and neural systems. Physiological noise is also unevenly distributed across brain regions, and it is modulated by cognitive processes (i.e., mental arithmetics). An accurate estimation of physiological noise is of utmost importance for the assessment of psychological function and related pathophysiology. Since noise may severely affect processing-derived metrics (e.g., PSD or complexity metrics), measurements in physiological systems and related statistics reported in the literature with no quantitative noise assessment are likely to be severely biased by underlying noise levels. The proposed noise estimation framework can be applied to any physiological time series, providing a noise measure that may strongly affect any existing biomarker derived from time-series.

Data Availability and Source Code

The MATLAB source code used to execute the proposed noise power estimation is available at https://github.com/AndScar/noise_estimation.

Appendix I
Approximate Entropy (ApEn)

The non-linear metric known as Approximate Entropy (ApEn) provides a measure of predictability for a given time series [25]. In mathematical terms, given a series $\{y_n\}_{n=1}^{N}$ consisting of N samples and a positive integer m, it is possible to embed the series into $\mathbb{R}^m$ and form vectors $Y_i = (y_i, \ldots, u_{i+m-1})$ with $i = 1, \ldots, N-m+1$. By selecting a distance d in $\mathbb{R}^m$ and a positive value r, it is possible to define $C_i^m(r) = \{\text{number of } j \text{ s.t. } d(Y_j, Y_i) < r\}$ and $\Phi^m(r) = (N-m+1)^{-1} \sum_i^{N-m+1} \log C_i^m(r)$, which provide the definition of the approximate entropy given by

$$\text{ApEn}(\{x_n\}_{n=1}^{N}, m, r) = \Phi^m(r) - \Phi^{m+1}(r).$$

The value of $\text{ApEn}(\{y_n\}_{n=1}^{N}, m, r)$ is always non-negative and reflects the proximity of the embedded vectors $\{Y_j\}_{j=1}^{N-m+1}$, where lower ApEn values correspond to higher predictability of the series.

References

[1] L. Cohen, "The history of noise [on the 100th anniversary of its birth]," *IEEE Signal Process. Mag.*, vol. 22, no. 6, pp. 20–45, Nov. 2005.

[2] M. Costa, A. L. Goldberger, and C.-K. Peng, "Multiscale entropy analysis of biological signals," *Phys. Rev. E*, vol. 71, no. 2, 2005, Art. no. 021906.

[3] E. Sejdić and L. A. Lipsitz, "Necessity of noise in physiology and medicine," *Comput. Methods Programs Biomed.*, vol. 111, no. 2, pp. 459–470, 2013.

[4] A. A. Faisal, L. P. Selen, and D. M. Wolpert, "Noise in the nervous system," *Nature Rev. Neurosci.*, vol. 9, no. 4, pp. 292–303, 2008.

[5] M. D. McDonnell and D. Abbott, "What is stochastic resonance? Definitions, misconceptions, debates, and its relevance to Biology," *PLoS Comput. Biol.*, vol. 5, no. 5, 2009, Art. no. e1000348.

[6] D. A. Rusakov, L. P. Savtchenko, and P. E. Latham, "Noisy synaptic conductance: Bug or a feature?," *Trends Neurosci.*, vol. 43, no. 6, pp. 363–372, 2020.

[7] C. M. Harris and D. M. Wolpert, "Signal-dependent noise determines motor planning," *Nature*, vol. 394, no. 6695, pp. 780–784, 1998.

[8] W. C. Stacey, M. T. Lazarewicz, and B. Litt, "Synaptic noise and physiological coupling generate high-frequency oscillations in a hippocampal computational model," *J. Neuriophysiol.*, vol. 102, no. 4, pp. 2342–2357, 2009.

[9] W. C. Stacey and D. M. Durand, "Synaptic noise improves detection of subthreshold signals in hippocampal CA1 neurons," *J. Neuriophysiol.*, vol. 86, no. 3, pp. 1104–1112, 2001.

[10] G. Deco and E. T. Rolls, "Decision-making and Weber's law: A neurophysiological model," *Eur. J. Neurosci.*, vol. 24, no. 3, pp. 901–916, 2006.

[11] G. Deco, E. T. Rolls, and R. Romo, "Stochastic dynamics as a principle of brain function," *Prog. Neurobiol.*, vol. 88, no. 1, pp. 1–16, 2009.

[12] K. D. Miller and T. W. Troyer, "Neural noise can explain expansive, power-law nonlinearities in neural response functions," *J. Neuriophysiol.*, vol. 87, no. 2, pp. 653–659, 2002.

[13] G. Valenza et al., "Complexity variability assessment of nonlinear time-varying cardiovascular control," *Sci. Rep.*, vol. 7, no. 1, pp. 1–15, 2017.

[14] A. A. Armoundas et al., "A stochastic nonlinear autoregressive algorithm reflects nonlinear dynamics of heart-rate fluctuations," *Ann. Biomed. Eng.*, vol. 30, no. 2, pp. 192–201, 2002.

[15] K. H. Chon et al., "Modeling nonlinear determinism in short time series from noise driven discrete and continuous systems," *Int. J. Bifurcation Chaos*, vol. 10, no. 12, pp. 2745–2766, 2000.

[16] V. Catrambone and G. Valenza, *Functional Brain-Heart Interplay: From Physiology to Advanced Methodology of Signal Processing and Modeling*. Cham, Switzerland: Springer, 2021.

[17] K. Sunagawa, T. Kawada, and T. Nakahara, "Dynamic nonlinear vago-sympathetic interaction in regulating heart rate," *Heart Vessels*, vol. 13, no. 4, pp. 157–174, 1998.

[18] G. Valenza et al., "Uncovering complex central autonomic networks at rest: A functional magnetic resonance imaging study on complex cardiovascular oscillations," *J. Roy. Soc. Interface*, vol. 17, no. 164, 2020, Art. no. 20190878.

[19] H.-F. Liu et al., "Noise robust estimates of the largest Lyapunov exponent," *Phys. Lett. A*, vol. 341, no. 1/4, pp. 119–127, 2005.

[20] T.-L. Yao et al., "Estimating the largest Lyapunov exponent and noise level from chaotic time series," *Chaos: An Interdiscipl. J. Nonlinear Sci.*, vol. 22, no. 3, 2012, Art. no. 033102.

[21] K. Urbanowicz and J. A. Hołyst, "Noise-level estimation of time series using coarse-grained entropy," *Phys. Rev. E*, vol. 67, no. 4, 2003, Art. no. 046218.

[22] T. Schreiber, "Determination of the noise level of chaotic time series," *Phys. Rev. E*, vol. 48, no. 1, 1993, Art. no. R13.

[23] A. Jayawardena, P. Xu, and W. K. Li, "A method of estimating the noise level in a chaotic time series," *Chaos: Interdiscipl. J. Nonlinear Sci.*, vol. 18, no. 2, 2008, Art. no. 023115.

[24] T. Sase et al., "Estimating the level of dynamical noise in time series by using fractal dimensions," *Phys. Lett. A*, vol. 380, no. 11/12, pp. 1151–1163, 2016.

[25] S. M. Pincus, "Approximate entropy as a measure of system complexity," *Proc. Nat. Acad. Sci.*, vol. 88, no. 6, pp. 2297–2301, 1991.

[26] A. Porta et al., "Are nonlinear model-free conditional entropy approaches for the assessment of cardiac control complexity superior to the linear model-based one?," *IEEE Trans. Biomed. Eng.*, vol. 64, no. 6, pp. 1287–1296, Jun. 2017.

[27] A. Porta et al., "Short-term complexity indexes of heart period and systolic arterial pressure variabilities provide complementary information," *J. Appl. Physiol.*, vol. 113, no. 12, pp. 1810–1820, 2012.

[28] A. Scarciglia et al., "Estimation of dynamical noise power in unknown systems," *IEEE Signal Process. Lett.*, vol. 30, pp. 234–238, 2023.
[29] A. Porta et al., "Progressive decrease of heart period variability entropy-based complexity during graded head-up tilt," *J. Appl. Physiol.*, vol. 103, no. 4, pp. 1143–1149, 2007.
[30] R. K. Udhayakumar, C. Karmakar, and M. Palaniswami, "Approximate entropy profile: A novel approach to comprehend irregularity of short-term HRV signal," *Nonlinear Dyn.*, vol. 88, pp. 823–837, 2017.
[31] P. Manneville and Y. Pomeau, "Different ways to turbulence in dissipative dynamical systems," *Physica D: Nonlinear Phenomena*, vol. 1, no. 2, pp. 219–226, 1980.
[32] A. L. Goldberger et al., "PhysioBank, PhysioToolkit, and PhysioNet: Components of a new research resource for complex physiologic signals," *Circulation*, vol. 101, no. 23, pp. e215–e220, 2000.
[33] H. Krum et al., "Effect of long-term digoxin therapy on autonomic function in patients with chronic heart failure," *J. Amer. College Cardiol.*, vol. 25, no. 2, pp. 289–294, 1995.
[34] "MIT-BIH arrhythmia database directory," Harvard-MIT Division of Health Sciences and Technology, Biomedical Engineering Center, Hypertext edition, 1997. [Online]. Available: https://archive.physionet.org/physiobank/database/html/mitdbdir/mitdbdir.htm
[35] G. Moody, "A new method for detecting atrial fibrillation using RR intervals," *Comput. Cardiol.*, vol. 10, pp. 227–230, 1983.
[36] J. Pan and W. J. Tompkins, "A real-time QRS detection algorithm," *IEEE Trans. Biomed. Eng.*, vol. BME-32, no. 3, pp. 230–236, Mar. 1985.
[37] L. Citi, E. N. Brown, and R. Barbieri, "A real-time automated point-process method for the detection and correction of erroneous and ectopic heartbeats," *IEEE Trans. Biomed. Eng.*, vol. 59, no. 10, pp. 2828–2837, Oct. 2012.
[38] W. Aziz et al., "Classification of heart rate signals of healthy and pathological subjects using threshold based symbolic entropy," *Acta Biologica Hungarica*, vol. 65, no. 3, pp. 252–264, 2014.
[39] I. Zyma et al., "Electroencephalograms during mental arithmetic task performance," *Data*, vol. 4, no. 1, 2019, Art. no. 14.
[40] S. Holm, "A simple sequentially rejective multiple test procedure," *Scand. J. Statist.*, vol. 6, pp. 65–70, 1979.
[41] C. A. Valentim, C. M. C. Inacio Jr, and S. A. David, "Fractal methods and power spectral density as means to explore EEG patterns in patients undertaking mental tasks," *Fractal Fractional*, vol. 5, no. 4, 2021, Art. no. 225.
[42] N. S. Pathan, M. Foysal, and M. M. Alam, "Efficient mental arithmetic task classification using wavelet domain statistical features and SVM classifier," in *Proc. Int. Conf. Elect., Comput. Commun. Eng.*, 2019, pp. 1–5.
[43] E. Magosso et al., "EEG alpha power is modulated by attentional changes during cognitive tasks and virtual reality immersion," *Comput. Intell. Neurosci.*, vol. 2019, pp. 1–18, 2019.
[44] M. Pertermann et al., "On the interrelation of 1/*f* neural noise and norepinephrine system activity during motor response inhibition," *J. Neurophysiol.*, vol. 121, no. 5, pp. 1633–1643, 2019.
[45] G. Valenza et al., "The central autonomic network at rest: Uncovering functional MRI correlates of time-varying autonomic outflow," *Neuroimage*, vol. 197, pp. 383–390, 2019.

Open Access provided by 'Università di Pisa' within the CRUI CARE Agreement